Acta Astronautica 95 (2014) 124–132

Contents lists available at ScienceDirect

Acta Astronautica

journal homepage: www.elsevier.com/locate/actaastro

Low-thrust trajectories for human missions to Ceres

Frank E. Laipert*, James M. Longuski

Purdue University, School of Aeronautics and Astronautics, 701 W. Stadium Ave., West Lafayette, IN 47907-2045, United States

ARTICLE INFO

Article history:
Received 13 February 2013
Received in revised form
18 October 2013
Accepted 2 November 2013
Available online 8 November 2013

Keywords:
Astrodynamics
Human space exploration
Low-thrust mission design
Ceres

ABSTRACT

A low-thrust trajectory design study is performed for a mission to send humans to Ceres and back. The flight times are constrained to 270 days for each leg, and a grid search is performed over propulsion system power, ranging from 6 to 14 MW, and departure V_∞, ranging from 0 to 3 km/s. A propulsion system specific mass of 5 kg/kW is assumed. Each mission delivers a 75 Mg payload to Ceres, not including propulsion system mass. An elliptical spiral method for transferring from low Earth orbit to an interplanetary trajectory is described and used for the mission design. A mission with a power of 11.7 MW and departure V_∞ of 3 km/s is found to offer a minimum initial mass in low Earth orbit of 289 Mg. A preliminary supply mission delivering 80 Mg of supplies to Ceres is also designed with an initial mass in low Earth orbit of 127 Mg. Based on these results, it appears that a human mission to Ceres is not significantly more difficult than current plans to send humans to Mars.

1. Introduction

Among potential destinations for humans to explore in the Solar System, Ceres stands out as one well-suited to human exploration. However, there has been little research that has addressed the problem of sending a human crew to Ceres. Benton has proposed a nuclear thermal rocket (NTR) vehicle design that could reach Ceres [1], but to our knowledge there has been little else on the matter. Other destinations have been subject to more study. Chief among them is Mars, which has long been considered the natural next step for exploration after the Moon [2–8]. We have also seen proposals to send astronauts to a near-Earth asteroid (NEA) [9] and to a Lagrange point in the Earth–Moon system [10]. While authors have looked at electric propulsion missions to Ceres at least as far back as 1971 [11], they have focused on robotic probes such as Dawn, which will reach Ceres in 2015 [12].

We aim to address this gap by presenting a low-thrust mission architecture that assesses the feasibility of a human mission to Ceres. Ceres possesses resources to aid in human exploration. Earth-based observations have demonstrated a high likelihood that significant quantities of water ice are present in the crust of Ceres [13,14]. When Dawn reaches Ceres in 2015, we will greatly expand our knowledge of the dwarf planet.

Reaching Ceres is a challenge because its very low gravity offers little assistance to a vehicle attempting to capture into orbit. Ceres' orbit also has an inclination of about 10.6°. At the same time, it lacks any appreciable atmosphere, so landing on Ceres would be similar to landing on the Moon or a large asteroid. On Mars, spacecraft can use the atmosphere to decelerate before landing, saving propellant. However, the atmosphere introduces significant uncertainty during landing, resulting in a target radius on the order of 10 km. On Ceres, thrusters must provide all deceleration, but in principle a more accurate landing should be possible.

We present a high-level mission concept to send human astronauts to Ceres and back. We focus on the low-thrust trajectory design but do not present a detailed

* Corresponding author. Tel.: +1 630 670 7548.
E-mail addresses: frank.laipert@outlook.com, flaipert@purdue.edu (F.E. Laipert), longuski@purdue.edu (J.M. Longuski).

0094-5765/$ - see front matter © 2013 IAA. Published by Elsevier Ltd. All rights reserved.
http://dx.doi.org/10.1016/j.actaastro.2013.11.003

Nomenclature

V_∞	hyperbolic excess velocity, km/s
e	eccentricity
Ω	longitude of the ascending node, rad
ω	argument of periapsis, rad
θ^*	true anomaly, rad
p	semi-latus rectum, km
L	true longitude $\Omega+\omega+\theta^*$, rad
i	inclination, rad
f	modified equinoctial element $e\cos(\omega+\Omega)$
g	modified equinoctial element $e\sin(\omega+\Omega)$
h	modified equinoctial element $\tan(i/2)\cos\Omega$
k	modified equinoctial element $\tan(i/2)\sin\Omega$
a_i	ith acceleration component, km/s^2
a	semi-major axis, km
β	steering angle, rad
m_{pl}	usable payload mass, Mg
m_f	total final mass at Ceres, Mg
α	propulsion system specific mass, kg/kW
P	spacecraft power, MW
μ_{p}	propellant tank mass factor
m_p	propellant mass, Mg
T	thrust, N
μ_{sc}	trajectory scaling factor
m_{leo}	initial mass in low Earth orbit, Mg
m_1	total mass after spiral, Mg
m_2	total mass after chemical escape, Mg

design of a transfer vehicle. However, estimates of the masses of the vehicles, the propellant costs, and the total initial mass in low Earth orbit (IMLEO) are provided. In addition, we provide a method to scale the mass results up or down to accommodate a payload mass different from the one assumed here. Our primary goal is to determine whether a human mission to Ceres is feasible given current technology and to identify which technological areas require further development.

2. Design methodology

2.1. Mission architecture overview

This mission presented here is built around the assumption of a two-vehicle, low-thrust propulsion concept. The first vehicle is the supply transfer vehicle (STV) and its mission is to deliver all supplies necessary to sustain the crew while on Ceres as well as any propellant or equipment required to return to Earth. We assume that its mission must be successfully completed before the astronauts depart.

The second vehicle is the crew transfer vehicle (CTV). We begin our mission analysis assuming that the CTV is already assembled in low-Earth orbit. It departs the Earth under the power of its electric propulsion using an elliptical spiral escape, performs an impulsive burn to achieve some departure V_∞, and uses electric propulsion to transfer to Ceres and back again to Earth. We will provide greater detail on each of these mission phases later in the paper.

2.2. Constraints

The need to protect the crew from a lengthy period of deep-space radiation exposure is the main factor driving the trajectory design for the crew mission. While there is great uncertainty in the effects of deep-space radiation on the human body, most authors indicate that such exposure would likely lead to fatal cases of cancer as well as other non-cancerous diseases [15]. We have constrained the Ceres-bound and Earth-bound legs to be no more than 270 days each, and the total time spent by the crew away from Earth on the Ceres mission to be no more than 2 years. For comparison, the NASA Mars Design Reference Architecture 5.0 (DRA5) specifies a maximum 180-day time of flight each way. While DRA5 has a total of six months less time in deep-space, the crew remains on the Martian surface for over a year, so the total time away from Earth is longer than the 2 year constraint we use here. A preliminary analysis indicated that a 270-day constraint provides a good balance between minimizing crew exposure to radiation while still requiring a reasonable IMLEO cost. We will return to the question of how this constraint affects IMLEO later in the paper.

Cucinotta and Durante [16] estimate that, given flight times similar to what we use here, the increased risk of developing a fatal case of cancer caused by exposure to deep-space radiation is about 4.0% for men and 4.9% for women, although these numbers are highly uncertain. While limiting flight times is one possible way to mitigate the risks faced by the crew, we acknowledge that the risk and uncertainty associated with deep-space radiation remains a major dilemma for human exploration of the Solar System.

Upon arrival at Ceres, V_∞ is constrained to be zero. This constraint is required because aerobraking is not possible at the atmosphere-free Ceres, and its gravity is so low that an impulsive capture maneuver is prohibitively expensive.

2.3. Technology assumptions

To make this mission possible while meeting the constraints, a nuclear electric propulsion (NEP) system is used throughout all stages of the mission. The low gravity and non-existent atmosphere on Ceres means that an impulsively propelled mission would require a significant amount of propellant to capture into orbit around Ceres and land. Unlike Mars, no aerocapture or aerobraking is possible. For these reasons, an electric propulsion system is selected because it allows the spacecraft to reach Ceres on a zero-V_∞ approach and spiral down to a low parking orbit. A nuclear power system is chosen over a solar-electric one because its specific mass is lower and its power output remains constant. For this study, we assume a propulsion system specific mass of $\alpha = 5$ kg/kW. This specific mass is in line with proposed methods of space-based nuclear power generation [17,18].

In addition to a nuclear power source, the mission requires an electric engine capable of meeting the thrust and specific impulse requirements. The VASIMR engine [19] is one such propulsion concept under development, and the magnetoplasmadynamic (MPD) thruster is another technology that has seen some study [20]. We assume a propulsive efficiency of 70%. As we will see, the architecture presented here—to minimize IMLEO—requires a thruster capable of processing 11.7 MW of input power at a constant specific impulse of 6800 s.

2.4. *Outbound trajectory design*

To minimize IMLEO for the mission, we perform a straightforward grid search of the trajectory design space with departure V_∞ and spacecraft power as our design variables. In creating this grid, we search over a range of 6–14 MW for power, in increments of 2 MW, and 0–3 km/s for V_∞, in increments of 1 km/s. This range yields a total of 20 possible design points. In the grid study, we proceed by first designing the interplanetary trajectory, next computing the ΔV for the Earth-orbit departure, and then designing an elliptical spiral that uses electric propulsion to escape low-Earth orbit. These steps are described in detail in Sections 2.4.1–2.4.3, as follows.

2.4.1. *Interplanetary trajectory*

At each design point, we use the software package MALTO (Mission Analysis Low-thrust Trajectory Optimization) to design a low-thrust trajectory. MALTO is developed and maintained by the Jet Propulsion Laboratory, and uses a direct method to produce optimal low-thrust trajectories [21]. For this study, we direct MALTO to produce a trajectory from Earth to Ceres that delivers 125 Mg (i.e. metric tons) of mass in 270 days, while minimizing the total departure mass. This 125 Mg includes the propulsion system mass. During the optimization process, the launch date is free, while the specific impulse is chosen from the range of 2000–8000 s. At the end of this step, we have the mass of the propellant required for the interplanetary leg and can compute the associated tank mass. We assumed a structural mass factor of 15%.

2.4.2. *Earth orbit departure*

Once we know the mass at the start of the interplanetary leg, we need to compute the mass of the chemical stage which places the transfer vehicle on an escape trajectory with the appropriate departure V_∞. The maneuver occurs at the perigee of a highly elliptical orbit, discussed in the next section. First, the escape ΔV is computed by taking the difference between the hyperbolic perigee velocity and the elliptical perigee velocity:

$$\Delta V = \sqrt{\frac{V_\infty^2}{2} + \frac{2\mu}{r_p}} - \sqrt{\frac{(1+e)\mu}{r_p}} \quad (1)$$

To achieve a 3 km/s V_∞ from an orbit with 0.95 eccentricity and 350 km perigee altitude, a ΔV of 543 m/s is required.

Then, the propellant mass is computed using the rocket equation, assuming an LH2/LOX propulsion stage with $I_{sp} = 450$ s:

$$m_0 = m_f \exp[\Delta V/(I_{sp} g_0)] \quad (2)$$

Again, we compute the structural mass assuming a factor of 15%.

2.4.3. *Elliptical spiral*

While it is possible to simply spiral away from the Earth with the electric propulsion engine by applying tangential thrust, this method would make it difficult for the crew to rendezvous with the transfer vehicle at the end of the spiral stage. The tangential spiral also makes it difficult to impart a departure V_∞ on the vehicle because the transfer from elliptical to hyperbolic orbit occurs at a point far away from Earth. A direct injection from low Earth orbit (LEO) to interplanetary transfer is also possible with a chemical propulsion stage, but this would be an inefficient use of propellant, especially for a spacecraft already equipped with a highly efficient electric propulsion system.

Instead, we employ an elliptical escape spiral similar to that proposed by Sweetser et al. [22]. Following their method, the spacecraft begins in LEO, and uses its electric propulsion system to spiral away from the Earth (without crew on board) with a steering law that keeps perigee constant while increasing apogee and eccentricity. An example of such a trajectory is shown in Fig. 1.

Because MALTO is not capable of computing the propellant required for an elliptical escape spiral, we use MATLAB to integrate the trajectory with the steering law from Sweetser et al., where we derive the steering law in terms of the modified equinoctial elements provided by Walker et al. [23]. The modified equinoctial elements can be obtained by a simple transformation of the classical orbital elements

$$p = a(1-e^2) \quad (3)$$

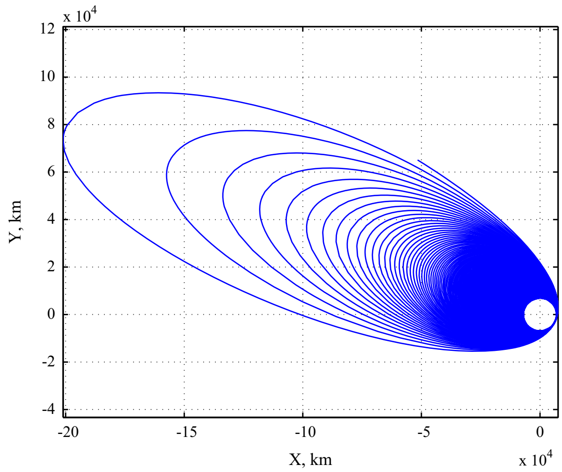

Fig. 1. This example shows the elliptical spiral trajectory of the crew transfer vehicle which maintains a constant perigee while using continuous low thrust to raise apogee. To avoid excessive exposure to radiation, the crew boards the crew transfer vehicle only after the orbit eccentricity reaches 0.95.

$$f = e\cos(\omega + \Omega) \tag{4}$$

$$g = e\sin(\omega + \Omega) \tag{5}$$

$$h = \tan(i/2)\cos\Omega \tag{6}$$

$$k = \tan(i/2)\sin\Omega \tag{7}$$

$$L = \Omega + \omega + \theta^* \tag{8}$$

Gauss' Planetary equations in terms of the modified equinoctial elements are

$$\dot{p} = \frac{2p}{w}\sqrt{\frac{p}{\mu}}a_\theta \tag{9}$$

$$\dot{f} = \sqrt{\frac{p}{\mu}}\left[a_r \sin L + [(w+1)\cos L + f]\frac{a_\theta}{w} - (h\sin L - k\cos L)\frac{g a_h}{w}\right] \tag{10}$$

$$\dot{g} = \sqrt{\frac{p}{\mu}}\left[-a_r \cos L + [(w+1)\sin L + g]\frac{a_\theta}{w} + (h\sin L - k\cos L)\frac{f a_h}{w}\right] \tag{11}$$

$$\dot{h} = \sqrt{\frac{p}{\mu}}\frac{s^2 a_h}{2w}\cos L \tag{12}$$

$$\dot{k} = \sqrt{\frac{p}{\mu}}\frac{s^2 a_h}{2w}\sin L \tag{13}$$

$$\dot{L} = \sqrt{\mu p}\left(\frac{w}{p}\right)^2 + \frac{1}{w}\sqrt{\frac{p}{\mu}}(h\sin L - k\cos L)a_h \tag{14}$$

where a_i are the components of the thrust acceleration in the orbit-fixed frame, s_L and c_L represent $\sin L$ and $\cos L$, respectively,

$$w = 1 + f\cos L + g\sin L \tag{15}$$

and

$$s^2 = 1 + h^2 + k^2 \tag{16}$$

To derive the steering law, we start by expressing the perigee radius in terms of the modified equinoctial elements:

$$r_p = a(1-e) = \frac{p}{1+\sqrt{f^2+g^2}} \tag{17}$$

where a is the orbit semi-major axis. Since we are holding perigee constant throughout the trajectory, we differentiate Eq. (17) and set the right hand side to zero:

$$\dot{r}_p = \left(1+\sqrt{f^2+g^2}\right)\dot{p} - pf\dot{f} - pg\dot{g} = 0 \tag{18}$$

Next, we substitute Eqs. (9)–(11) into Eq. (18) and group together the coefficients of the acceleration components. The a_h terms cancel out leaving us with

$$(-fs_L + gc_L)a_r + \left\{\frac{2(e+e^2)}{w} - \frac{f}{w}[(w+1)c_L + f] - \frac{g}{w}[(w+1)s_L + g]\right\}a_\theta = 0 \tag{19}$$

The coefficient of the a_θ term can then be simplified using Eq. (15) and noting that $e^2 = f^2 + g^2$

$$(-f\sin L + g\cos L)a_r + \frac{1}{w}[2e + 2e^2 - (w+1)(f\cos L + g\sin L) - (f^2+g^2)]a_\theta = 0 \tag{20}$$

$$(-f\sin L + g\cos L)a_r + \frac{1}{w}\left[e^2 + 2e - (w^2 - 1)\right]a_\theta = 0 \tag{21}$$

The steering angle, β, is defined here as the angle from the local horizon to the thrust vector, and is given by

$$\tan\beta = \frac{a_r}{a_\theta} = \frac{e^2 + 2e - w^2 + 1}{w(f\sin L - g\cos L)} \tag{22}$$

In the form originally given by Sweetser et al. [22], the steering law produced a singularity when the spacecraft reached periapse and apoapse. This singularity required the user to modify the steering law slightly when implementing it numerically. Using the form presented in Eq. (22), numerical difficulties did not occur when propagating a trajectory using the elliptical spiral steering law.

While it is not obvious upon examining the control law as presented here, intuitively we can surmise that when the spacecraft is at perigee, thrust should be in the tangential direction, and when the spacecraft is near apogee, thrust cannot be in the tangential direction, or else it will raise perigee. So in general, the thrust direction for true anomalies near 180° will tend towards the radial direction. However, radial thrust does not increase the energy of the orbit and is an inefficient use of propellant if we want the spacecraft to escape. Therefore, we can save propellant by setting a maximum true anomaly, θ_{max}, beyond which the spacecraft will coast. It will resume thrusting after it passes $2\pi - \theta_{max}$. While this modification to the control law does save propellant, it comes at the expense of increased time in the elliptical spiral stage. For this mission we have found $\theta_{max} = 60^\circ$ to strike a good balance between propellant savings and increased time of flight.

We note that there may be a better and more efficient way to increase apogee and eccentricity than the Sweetser method, however the goal of this paper is not to find the optimal solution, but a practical one that demonstrates the feasibility of the human mission to Ceres we are proposing here. There may exist a steering law that achieves the same target orbit as the elliptical spiral used here, but at a reduced propellant cost. Additionally, the Moon may be used as a gravity-assist body during the escape phase. These escape strategies should only reduce propellant usage, and hence IMLEO, for the mission. Because this study is intended as a high-level feasibility analysis, we will proceed with the non-optimal escape strategy which, as we will see, is adequate for the mission given our assumptions.

The CTV travels on a spiral trajectory for about 2 years to reach a highly eccentric orbit with $e = 0.95$ and a perigee altitude of 350 km. (Subsequently, the crew is launched in a small capsule to rendezvous with and board the CTV.)

At each point in the grid study, we compute the propellant mass (and tank mass) required to bring the transfer vehicle and chemical departure stage from LEO to the highly elliptical orbit. This computation is done by backwards propagation from an elliptical orbit ($e=0.95$) with the final mass required for the impulsive escape maneuver to a circular orbit of 350 km altitude. The initial mass (computed at the end of the backward propagation) is a reasonable estimate of the total IMLEO required to complete the mission.

2.5. Computing payload mass

While each trajectory delivers 125 Mg to Ceres, the payload mass varies because we must deduct the inert mass of the propulsion system from the final mass:

$$m_{pl} = m_f - \alpha P - \mu_p m_p \tag{23}$$

The propulsion system inert mass includes the nuclear reactor, the thrusters, and the propellant tanks. So while high-power missions will tend to use less propellant than low-power missions, they will require a larger power system mass. These competing effects generally result in an optimum propulsion power level that balances propellant mass with inert mass.

2.6. Scaling the results

MALTO is able to compute a trajectory that minimizes initial mass given a fixed final mass, but it is not able to do the same given a fixed payload mass. Because of this, the set of trajectories produced by the grid search are unequal in the sense that they do not deliver the same usable payload to Ceres. To account for this fact, we adopt the scaling method presented by Landau et al. [24]. This method allows the mission planner to take a trajectory that delivers a particular payload mass, m_{pl}, and scale it up in such a way that the scaled trajectory follows the same course and has the same time of flight, but delivers a new payload mass, m^*_{pl}, to the destination. The first step is to compute the scaling factor:

$$\mu_{sc} = m^*_{pl}/m_{pl} \tag{24}$$

Then, this factor can be used to scale up other key mission parameters, such as spacecraft power and thrust:

$$P^* = \mu_{sc} P, \quad T^* = \mu_{sc} T \tag{25}$$

We are also able to scale up the propellant masses and total IMLEO for the trajectory:

$$m^*_p = \mu_{sc} m_p, \quad m^*_{LEO} = \mu_{sc} m_{LEO} \tag{26}$$

For each design point in the grid search, we have scaled the final payload mass to 75 Mg and adjusted the spacecraft power for each design accordingly.

2.7. Return trajectory

To design the return trajectory, we again use MALTO. In a manner similar to designing the outbound trajectory, we fix the mass at Earth arrival to be 125 Mg, constrain the flight time to be no more than 270 days, and direct MALTO to minimize the propellant mass. We assume that the transfer vehicle restocks the propellant it needs for the return leg at Ceres. The return propellant may either be delivered directly in the supply mission, or it may be produced by an in situ propellant facility delivered on the supply mission. Here we assume that it is delivered on the supply mission. Upon return to Earth, the arrival V_∞ is constrained to less than 4.5 km/s, which results in an atmospheric entry velocity of around 12 km/s. For reference, the Apollo entry velocity was about 11 km/s [25]. The ability to use the Earth's atmosphere to capture significantly reduces the propellant required on the return trip compared to the outbound trip.

2.8. Supply mission

Before any mission carrying astronauts departs for Ceres, a mission to bring supplies and resources to Ceres should have been successfully completed. We perform another grid search to estimate the IMLEO of such a cargo mission in a manner much the same as that of the human mission. The supply mission analysis is different from the human mission in that (1) the time of flight is constrained to 2 years and (2) the grid search is one-dimensional over power.

Departure V_∞ is constrained to be zero. This constraint allows the supply vehicle to depart Earth on a circular spiral, which is possible because the absence of crew removes the need for the elliptical spiral. The power level is varied from 1 to 3 MW in increments of 0.5 MW in search of an optimal solution. Our search range is lower than that of the human mission because the longer time of flight allows for lower thrust and lower power.

3. Results

3.1. Human mission

Table 1 contains the complete listing of results from the outbound grid search. Of the original 20 design points, 4

Table 1
Results from the grid search before scaling where masses are in Mg (metric tons).

P (MW)	V_∞ (km/s)	m_{leo}	m_1	m_2	m_{pl}	m_{pl}/m_{leo}	Return m_p	m^*_{leo}
6	3	454	394	340	63	0.14	120.0	542
8	1	391	347	330	54	0.14	87.4	541
8	2	320	290	266	64	0.20	72.7	376
8	3	295	271	234	69	0.23	64.8	323
10	0	318	289	279	52	0.16	63.5	459
10	1	273	252	240	58	0.21	54.2	354
10	2	253	235	216	61	0.24	49.7	309
10	3	246	230	199	64	0.26	46.0	289[a]
12	0	253	235	227	50	0.20	45.6	381
12	1	230	216	206	53	0.23	40.4	326
12	2	221	209	192	55	0.25	37.3	302
12	3	221	210	181	57	0.26	35.1	292
14	0	222	210	202	43	0.19	35.5	383
14	1	209	198	189	45	0.22	32.3	345
14	2	203	194	178	47	0.23	30.3	324
14	3	207	198	171	48	0.23	29.3	323

[a] Best performing case, that is, lowest m^*_{leo} for fixed payload mass.

were found to be infeasible given the mission constraints, leaving us with 16 design points. Except for the last column, the results in Table 1 are not scaled and all deliver the same final mass of 125 Mg to Ceres. They differ in payload mass because of the different propulsion system masses, but our interest is in delivering a 75 Mg payload. In Table 1, m_1 and m_2 refer to the total spacecraft mass after the elliptical spiral and after the impulsive escape burn, respectively. A useful measure of merit to compare the different missions is the ratio of payload mass to IMLEO. We found that the missions which made the most efficient use of the total initial mass were the same ones that required the least initial mass when all the design points were scaled. The final scaled IMLEO is given in the final column as m^*_{leo}. For example, in the first row of Table 1, we compute $\mu_{sc} = 75/63 = 1.194$, and then multiply m_{leo} by μ_{sc} to get $m^*_{leo} = 542$ Mg. Similarly, $P^* = 6 \times 1.194 = 7.16$ MW, $m^*_1 = 470$ Mg and $m^*_2 = 406$ Mg (V_∞ is not scaled, so $V_\infty = 3$ km/s).

In Fig. 2, we have taken the data from Table 1 and scaled the masses so that each design point in the plot delivers 75 Mg of usable payload to Ceres. The minimum solution has a power of 11.2 MW (which was scaled up from 10 MW) and a departure V_∞ from Earth of 3 km/s. Following the trend shown on the plot, a higher departure V_∞ may lower total IMLEO further, but the returns appear to diminish.

A local minimum appears along the power dimension because there is a balance between the increased efficiency at higher power levels and the increased mass of the power system itself. MALTO is allowed to choose the optimum I_{sp} (within limits) at each design point, and at higher power levels it increases I_{sp} to decrease propellant consumption while keeping acceleration the same for the different trajectories. A similar effect occurs with departure V_∞, where at higher departure velocities, a higher I_{sp} can be used since the total change in orbital energy during the transfer is smaller and less thrust is required.

3.2. Scaling accuracy

Because our result depends on the accuracy of the scaling method we applied, we validate the method by re-running a selection of design points in MALTO using the scaled final mass as our delivered mass to Ceres (rather than the 125 Mg used in the original search) as well as the scaled power level. We then compute the IMLEO by computing the propellant and structural mass required to depart Earth with the elliptical spiral and chemical escape maneuver, as described in Section 2. Performing the second analysis with the 10 MW, 3 km/s V_∞ case results in an IMLEO of 289 Mg, while simply scaling the IMLEO from the initial run results in a value of 288 Mg, a difference of only 0.3%. Performing the same check on the second best design point (12 MW, 3 km/s) resulted in the same discrepancy of 0.3%. We conclude that the accuracy of the scaling method is sufficient for the purpose of this study.

3.3. Supply mission

The results of the supply mission analysis, shown in Fig. 3, indicate that a minimum IMLEO is obtained using a power source of about 2.45 MW. This mission has an interplanetary flight time of 2 years and a circular spiral to depart Earth and capture into Ceres orbit. The mission brings 80 Mg of supplies and return propellant to Ceres and has an IMLEO of 127 Mg.

The supply mission analysis did not examine the effect of departure V_∞. Since the time constraints and human considerations are far less stringent on the supply mission, a circular spiral is used instead. The circular spiral precludes the use of a chemical escape booster since it cannot leverage a high perigee velocity. The propellant required for the circular spiral stage is computed by MALTO and does not require a separate analysis.

Because it is not evident that a circular escape spiral is more economical than an elliptical escape (as used in the human mission), we perform a simple trade study using an

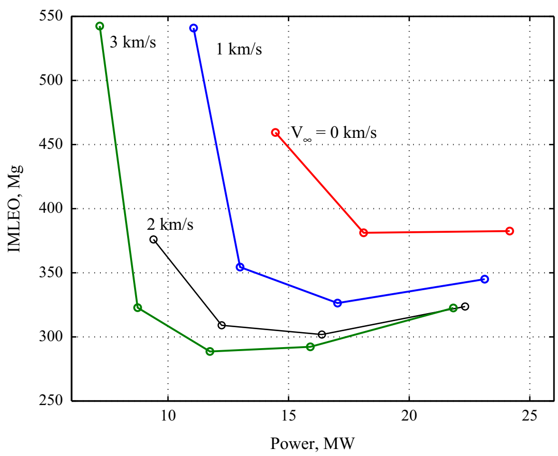

Fig. 2. The crew mission study reveals a minimum total IMLEO (after scaling) at a power level of 11.7 MW and departure V_∞ of 3 km/s. The numbers at the left end of each curve indicate the departure V_∞.

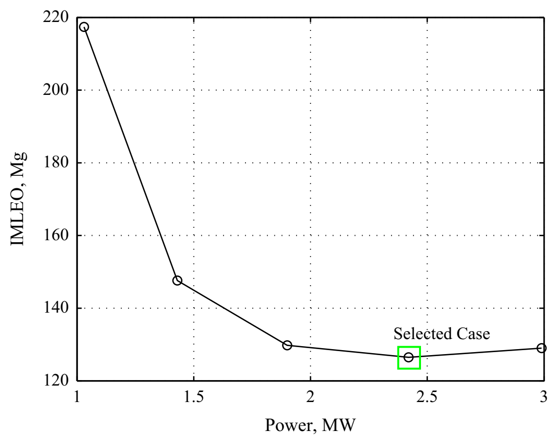

Fig. 3. The supply mission study reveals a local minimum IMLEO at about 2.45 MW. These results are scaled so that all the design points deliver an 80 Mg supply payload to Ceres.

elliptical spiral escape for the supply mission to examine the effect of this escape method on IMLEO. Using the elliptical escape with no coast arc around apogee, we find that the minimum IMLEO occurs again at P=2.45 MW, with an IMLEO of 132 Mg and a flight time of 345 days. This case is both more massive and takes longer than the circular escape method, which has an IMLEO of 127 Mg and escape time of 214 days. We may reduce propellant consumption at the expense of increased flight time by setting a maximum true anomaly past which the spacecraft does not thrust, as described previously. Setting $\theta_{max} = 135^\circ$ results in an IMLEO of 124 Mg—a savings of 3 Mg over the circular spiral. However these savings come at a cost of a 621 day flight time. Lowering θ_{max} to 60° reduces IMLEO to 121 Mg, but the flight time increases to an unacceptable duration of 2318 days.

3.4. Design selection

After performing the grid search, we have identified a near-optimal design point for a human mission to Ceres. As we noted earlier, the selected design has an IMLEO of 289 Mg and a power of 11.7 MW and delivers a 75 Mg payload to Ceres. In Table 2 we can see the mass budget for the design after scaling is applied. For the electric propulsion system, the inert mass fraction is 45%. For the overall mission, 47% of the IMLEO is propellant, 27% is inert mass, and 26% is payload. The total IMLEO for the crew mission is 289 Mg, while for the supply mission the total IMLEO is 127 Mg. The combined IMLEO then, with an arbitrary margin of 10%, is 458 Mg. For comparison, the total on-orbit mass of the International Space Station is 450 Mg. We also note that four heavy lift launch vehicles would suffice to enable this mission.

In Table 3 we have the time line for the full mission. The initial supply mission launches in October 2026, the crew mission departs in August 2030, and the crew returns to Earth in May 2032. Since the mission architecture does not involve any gravity-assist bodies, launch opportunities should repeat around the time when Ceres passes the ascending or the descending node, or roughly every 2.3 years.

Fig. 4 depicts the trajectory and events of the crew mission, including the outbound trajectory, the stay on Ceres, and the return trajectory. From a three-dimensional version of the trajectory plot, we learn that the surface operations on Ceres occur when Ceres is near the ecliptic plane and the Sun is between the Earth and the Ceres. A simple analysis for our particular mission showed a minimum Sun–Earth–CTV angle of 2.15°, which occurs when the CTV is at Ceres. Depending on the communications architecture used, extra communications infrastructure, such as an Earth-trailing satellite, may be required to ensure an uninterrupted link.

Table 2
Mass table for selected design.

Item	Mass (Mg)
Spiral propellant	18.3
Chemical escape propellant	31.3
Transfer propellant	87.4
Chemical escape structure	5.52
Transfer structure	13.0
Propulsion inert mass	58.7
Payload	75.0
Total	289

3.5. Time-of-flight trade study

As we noted earlier, the question of how to constrain the TOF is not easily answered because of the great uncertainty in how the deep-space radiation environment affects the human body. Ideally, we need a way to directly compute the risk of losing a crew member (as a result of exposure to deep-space radiation on any given mission) so we could set a TOF constraint directly based on that risk. However until we are able to perform such an analysis, we resort to simply constraining the time of flight to a feasibly low value.

In Fig. 5, we present the results of a trade study where we vary the time-of-flight constraint while keeping the payload mass and power constant. MALTO was allowed to adjust the launch and arrival dates, the I_{sp}, and the stay time on Ceres to minimize the initial mass. The I_{sp} was bounded between 2000 and 8000 s, and the stay time on Ceres was set to a lower bound of 90 days. TOF constraints

Table 3
Time line of mission events.

Event	Date (m/d/y)
STV launches and begins spiral	10/19/2026
Supply mission departs	5/27/2027
Supply mission arrives	5/21/2029
Crew vehicle begins spiral	Before 7/19/2028[a]
CTV begins interplanetary leg	8/6/2030
CTV arrives on Ceres	5/3/2031
CTV departs Ceres	8/23/2031
CTV returns to Earth	5/19/2032

[a] Spiral phase takes 748 days to complete as designed.

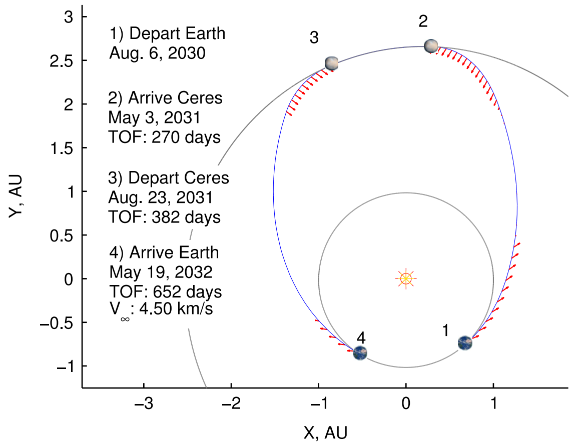

Fig. 4. (1) August 6, 2030: crew departs Earth. (2) May 3, 2031: crew arrives at Ceres. (3) August 23, 2031: crew departs Ceres. (4) May 19, 2032: crew returns to Earth. Total mission time is 652 days or 1.79 years.

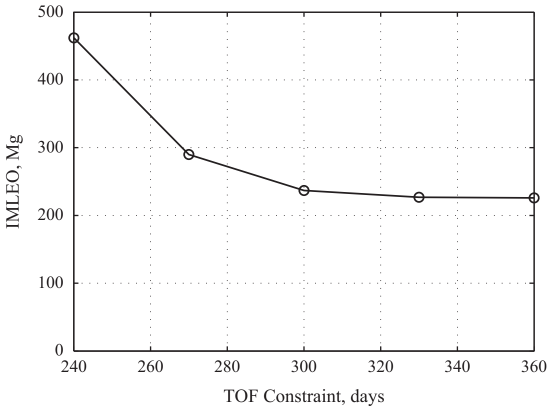

Fig. 5. The IMLEO increases dramatically for TOF constraints lower than 240 days. For the case study in this paper a TOF of 270 days is assumed.

ranged from 240 days to 360 days in increments of 30 days. For each TOF constraint setting, we calculated the total IMLEO in the same manner as with the initial grid search.

What we see is that the 270-day TOF constraint appears adequate given the assumptions of the trade study. The phasing of the mission is a likely factor preventing significant reductions in IMLEO for longer TOF constraints. MALTO is given freedom to choose the launch dates in the mission, and it has chosen the dates such that the spacecraft arrives and departs Ceres while the dwarf planet is near the ascending node of its orbit. Arriving at Ceres while it is near the ascending node means that most of the plane change required to reach Ceres can be performed at a greater heliocentric distance, where less propellant is needed. Subsequently, when the TOF constraint is loosened, MALTO reduces the time spent on the surface of Ceres so that the arrival still occurs near the ascending node of the orbit, until the lower constraint on stay time (30 days) is reached. When no more time can be taken away from the surface operations and diverted to the transfer, the launch dates must be altered and there is less benefit to an increased TOF.

A more thorough analysis could be achieved by performing an entirely new grid search over power and departure V_∞ for each constraint, in essence adding the TOF constraint as a third design variable. However, in general it is reasonable to assume that a shorter TOF constraint will require more propellant and higher IMLEO, so the question becomes whether the mass savings of a longer TOF can be reassigned to bolster radiation shielding such that overall risk to the astronauts is reduced. We must, of necessity, leave this question open pending a reliable method of quantifying the radiation health risk.

4. Discussion

4.1. Key technologies to develop

The primary technology enabling a human mission to Ceres is a nuclear power system capable of generating 11.7 MW of power with a specific mass of 5 kg/kW. A mission may be feasible with a smaller power system of around 8–9 MW, however more propellant and a higher IMLEO would be required. In addition to the power system itself, an electric propulsion technology capable of converting that power into thrust with an efficiency of about 70% is needed.

4.2. In situ resource utilization vs pre-delivered propellant

Given that significant quantities of water ice exist in the regolith of Ceres (i.e. between 3% and 20% of the mass of the regolith), it is possible that a mission to Ceres could use that water to produce propellant for the return mission through electrolysis. The option of in situ resource utilization would be attractive if the cost of sending the required equipment would be less than that of sending return propellant to Ceres. The in situ propellant could feed a liquid-oxygen, liquid-hydrogen chemical propulsion system, or it may serve as the propellant for an electric system in the form of H_2. In the latter case, the electric propulsion system would be limited to high specific impulse because of the very low atomic mass of hydrogen.

5. Conclusion

We can draw the following conclusions from this mission design study.

1. A human mission to Ceres could be made feasible with the appropriate investment in propulsion and in-space power technology. Given the assumptions used here, the total IMLEO, with a 10% margin, would be 458 Mg. The mission architecture presented here would deliver a total of 155 Mg of payload to Ceres over two missions. Four heavy-lift launch vehicles would suffice to carry out such a mission.
2. Nuclear electric propulsion technology enables human exploration at Ceres because it has a relatively low specific mass (i.e. about 5 kg/kW) and it avoids a costly impulsive capture maneuver at Ceres. Electric propulsion technologies capable of processing input power up to 11.7 MW (or more) should be further developed to open the possibility of exploring Ceres.
3. Total mission times of less than 2 years (for the crew) are possible with nuclear electric propulsion. In the absence of a proven method of blocking deep-space radiation, limiting mission times is the best way to limit the danger to the crew.

References

[1] M.G. Benton, Spaceship discovery—NTR vehicle architecture for human exploration of the solar system, in: 45th AIAA/ASME/SAE/ASEE Joint Propulsion Conference and Exhibit, AIAA 2009–5309, 2009.
[2] G. Walberg, How shall we go to Mars?: a review of mission scenarios, J. Spacecr. Rockets 30 (1993) 129–139.
[3] B.G. Drake, Human Exploration of Mars Design Reference Architecture 5.0, Technical Report NASA-SP-2009-566, NASA, 2009.
[4] D.F. Landau, J.M. Longuski, Trajectories for human missions to Mars, part 1: impulsive transfers, J. Spacecr. Rockets 43 (2006) 1035–1042.
[5] D.F. Landau, J.M. Longuski, Trajectories for human missions to Mars, part 2: low-thrust transfers, J. Spacecr. Rockets 43 (2006) 1043–1047.

[6] D. Landau, Strategies for the sustained human exploration of mars (Ph.D. thesis), Purdue University, 2006.
[7] D.F. Landau, J.M. Longuski, Comparative assessment of human–Mars-mission technologies and architectures, Acta Astronaut. 65 (2009) 893–911.
[8] J.M. Salotti, Simplified scenario for manned Mars missions, Acta Astronaut. 69 (2011) 266–279.
[9] B.W. Barbee, T. Esposito, E. Pinon III, S. Hur-Diaz, R.G. Mink, D.R. Adamo, A comprehensive ongoing survey of the near-Earth asteroid population for human mission accessibility, in: AIAA Guidance, Navigation, and Control Conference, Toronto, Canada, AIAA 2010–8368, 2010.
[10] B. Sherwood, M. Adler, L. Alkalai, G. Burdick, D. Coulter, F. Jordan, F. Naderi, L. Graham, R. Landis, B. Drake, S. Hoffman, J. Grunsfeld, B.D. Seery, Flexible-path human exploration, in: AIAA SPACE 2010 Conference and Exposition, AIAA 2010–8607, 2010.
[11] D.R. Brooks, Solar electric missions to Ceres, J. Spacecr. 8 (1971) 889–890.
[12] C.T. Russell, F. Capaccioni, A. Coradini, M.C.D. Sanctis, W.C. Feldman, R. Jaumann, H.U. Keller, T.B. McCord, L.A. McFadden, S. Mottola, C. M. Pieters, T.H. Prettyman, C.A. Raymond, M.V. Sykes, D.E. Smith, M. T. Zuber, Dawn mission to Vesta and Ceres, Earth Moon Planets 101 (2007) 65–91.
[13] L.A. Lebofsky, M.A. Feierberg, A.T. Tokunaga, H.P. Larson, J.R. Johnson, The 1.7- to 4.2−μm spectrum of asteroid 1 Ceres: evidence for structural water in clay minerals, Icarus 48 (1981) 453–459.
[14] F.P. Fanale, J.R. Salvail, The water regime of asteroid (1) Ceres, Icarus 82 (1989) 97–110.
[15] M.-H.Y. Kim, G.D. Angelis, F.A. Cucinotta, Probabilistic assessment of radiation risk for astronauts in space missions, Acta Astronaut. 68 (2011) 747–759.
[16] F.A. Cucinotta, M. Durante, Cancer risk from exposure to galactic cosmic rays: implications for space exploration by human beings, Lancet Oncol. 7 (2006) 431–435.
[17] R.J. Litchford, L.J. Bitteker, J.E. Jones, Prospects for Nuclear Electric Propulsion Using Closed-Cycle Magnetohydrodynamic Energy Conversion, Technical Report TP-2001-211274, NASA, Marshall Space Flight Center, 2001.
[18] R.J. Litchford, N. Harada, Multi-MW closed cycle MHD nuclear space power via nonequilibrium He/Xe working plasma, in: Proceedings of Nuclear and Emerging Technologies for Space 2011, 2011.
[19] E.A. Bering III, B.W. Longmier, M. Ballenger, C.S. Olsen, J.P. Squire, F.R. C. Diaz, Performance studies of the VASIMR VX-200, in: AIAA Aerospace Sciences Meeting and Exhibit, 2011.
[20] J.S. Sovey, M.A. Mantenieks, Performance and lifetime assessment of magnetoplasmadynamic arc thruster technology, J. Propuls. 7 (1991) 71–83.
[21] J.A. Sims, P.A. Finlayson, E.A. Rinderle, M.A. Vavrina, T.D. Kowalkowski, Implementation of a low-thrust trajectory optimization algorithm for preliminary design, in: AIAA/AAS Astrodynamics Specialist Conference and Exhibit, 2006.
[22] T.H. Sweetser, M.J. Cherng, P.A. Penzo, P.A. Finlayson, Watch out, it's hot! Earth capture and escape spirals using solar electric propulsion, in: AAS/AIAA Astrodynamics Specialist Conference and Exhibit, 2001.
[23] M. Walker, B. Ireland, J. Owens, A set of modified equinoctial orbit elements, Celest. Mech. 36 (1985) 409–419.
[24] D. Landau, J. Chase, T. Randolph, P. Timmerman, D. Oh, Electric propulsion system selection process for interplanetary missions, J. Spacecr. Rockets 48 (2011) 467–476.
[25] C.A. Graves, J.C. Harpold, Apollo Experience Report—Mission Planning for Apollo Entry, Technical Report TN D-6725, NASA, 1972.